Chemistry
A European Journal

Chemistry Europe
European Chemical
Societies Publishing

Title: Hybrid Eu(III) Coordination luminophore Standing on Silica Nanoparticles By Two Legs for Enhanced Luminescence

Authors: Teng Zhang, Yuichi Kitagawa, Ryoma Moriake, Pedro Paulo Ferreira da Rosa, Md Jahidul Islam, Tomoki Yoneda, Yasuhide Inokuma, Koji Fushimi, and Yasuchika Hasegawa

To be cited as: *Chem. Eur. J.* 10.1002/chem.202102156

Link to VoR: https://doi.org/10.1002/chem.202102156

WILEY-VCH

WILEY-VCH

Hybrid Eu(III) Coordination luminophore Standing on Silica Nanoparticles By Two Legs for Enhanced Luminescence

Dr. Teng Zhang,[a] Dr. Yuichi Kitagawa,[a, b] Ryoma Moriake,[c] Pedro Paulo Ferreira da Rosa,[c] Dr. Md Jahidul Islam,[a] Dr. Tomoki Yoneda,[b] Prof. Yasuhide Inokuma,[a, b] Dr. Koji Fushimi[b] and Prof. Yasuchika Hasegawa*[a,b]

[a] Institute for Chemical Reaction Design and Discovery (WPI-ICReDD), Hokkaido University, Sapporo, Hokkaido 001-0021, Japan.
[b] Faculty of Engineering, Hokkaido University, Sapporo, Hokkaido 060-8628, Japan.
[c] Graduate School of Chemical Sciences and Engineering, Hokkaido University, Sapporo, Hokkaido 060-8628, Japan.
E-mail: hasegaway@eng.hokudai.ac.jp

Abstract: In this study, we demonstrated a two-legs standing-up molecular design method for mono-chromatic and bright red luminescent Ln(III)-silica nanomaterials. A novel Eu(III)-silica hybrid nanoparticle using double binding TPPO-Si(OEt)$_3$ (TPPO: triphenyl phosphine oxide) linker were developed. The TPPO-Si(OEt)$_3$ was determined by ^{1}H, ^{31}P, ^{29}Si NMR spectroscopy and single-crystal X-ray analysis. Luminescent Eu(hfa)$_3$ and Eu(tfc)$_3$ parts (hfa: hexafluoroacetylacetonate, tfc: 3-(trifluoromethylhydroxymethylene)camphorate) were fixed on the TPPO-Si(OEt)$_3$ modified silica nanoparticles, producing in Eu(hfa)$_3$(TPPO-Si)$_2$-SiO$_2$ and Eu(tfc)$_3$(TPPO-Si)$_2$-SiO$_2$, respectively. The Eu(hfa)$_3$(TPPO-Si)$_2$-SiO$_2$ exhibited higher intrinsic luminescence quantum yield (93%) and longer emission lifetime (0.98 ms), which is much larger than those of previously reported Eu(III)-based hybrid materials. Eu(tfc)$_3$(TPPO-Si)$_2$-SiO$_2$ also showed extra-large intrinsic emission quantum yield (54%), although the emission quantum yield for the precursor Eu(tfc)$_3$(TPPO-Si(OEt)$_3$)$_2$ was found to be 39%. These results confirmed that the TPPO-Si(OEt)$_3$ linker is a promising candidate for development of Eu(III)-based luminescent materials.

Introduction

Luminescent molecular materials attract considerable attention not only due to their practical applications in lamps, lasers and displays,[1] but also widely used in biomedicine, optoelectronic devices, and sensors.[2-5] Thus, various types of luminescent molecular materials using organic dyes,[6,7] transition metal compounds,[8,9] and lanthanide-based complexes[10-12] have been developed in the field of material chemistry. To improve physical properties and chemical stabilities of the luminescent molecular materials, many research efforts have focused on hybrid nanomaterials decorated with luminescent molecules.[13-15] The hybrid luminescent nanomaterial can combine both advantages of the solid matrix (rigidity and thermal stability) and the molecular compound (flexibility for molecular design). Their physicochemical properties depend on nature of the substrate (silica, zirconia and zinc oxide) and the surface conditions. Nanomaterial attached with noble metals (gold, silver, platinum, ruthenium, and/or iridium) represent a class of hybrid luminescent material that have been well studied,[16-19] and applied in probes, bioimaging, and catalysis.[20-22] In addition, organic ligand-functionalized nanomaterials for enhancing luminescence were also investigated recently, such as upconversion nanoparticles, quantum dots, and the nanoMOFs.[23-25]

Here, we focus on the lanthanide(III)-coordinated nanomaterial as a bright luminophore. The Ln(III)-coordinated based materials show characteristic luminescence with sharp spectral shape (FWHM < 10 nm), large stokes shift and long emission lifetime (> micro seconds) originated from *4f-4f* forbidden transtions.[10,26] In the past decade, various types of Ln(III)-based materials such as sol-gel materials, polymers, and mesoporous materials have been developed.[27-30] Binnemans and Gunnlaugsson reported on Ln(III) complex-based sol-gel and polymer derived luminescent materials.[31,32] An Eu/Tb(III) complex-based sol-gel material with reversible stimuli-responsive properties was also achieved.[33] The Ln(III)-modified mesoporous materials were obtained by grafting Ln(III) complex onto a mesoporous matrix, for example, immobilizing lanthanide β-diketone or pyridine complexes onto the SBA-15, MCM-41, and silica hosts were fully investigated.[30,34,35] Even though their thermal stability enhanced, the emission quantum yields of previous Ln(III)-coordinated materials are smaller than those of corresponding pure Ln(III) complexes. In this context, novel conceptual design for Ln(III)-based luminescent materials is required.

In previously reported Ln(III)-based materials, the Ln(III) complexes were functionalized on the inorganic matrix surface with one binding site (Figure 1a: L2 joint),[36-38] in this case, the flexible vibration of the organic ligands can decrease of Ln(III) emission quantum yield. Here, we demonstrate a novel fixation method, taking advantage of an Eu(III) complex with organic ligand covalently bonded to the silica nanoparticles through two binding sites as support (Figure 1b: L2' joins). Fixation of Eu(III) complex on the covalent rigid Si-O-Si polymeric network structures of the silica nanoparticles surface with two binding sites, can promote effective suppression of the vibrational relaxation process of the excited organic ligand, resulting in enhanced luminescence performance. As reported in our previous work, the hfa has low vibrational frequency for decreasing the non-radiative rate constant,[39] and TPPO can formation of antisymmetric structure for increasing of the radiative rate constant[40,41]. Therefore, in this study, we synthesized a new triphenylphosphine oxide compound TPPO-Si(OEt)$_3$ and identified by ^{1}H, ^{31}P, ^{29}Si NMR spectroscopies and single-crystal X-ray analysis. Using Eu(hfa)$_3$ complex with TPPO-Si(OEt)$_3$ ligand covalently bonded to the silica nanoparticle through two binding sites, we developed a nano-luminophore Eu(hfa)$_3$(TPPO-Si)$_2$-SiO$_2$ (Figure 1c). It exhibited higher intrinsic luminescence quantum yield (93%) and longer emission lifetime (0.98 ms), which is much larger than

10.1002/chem.202102156

those of previous Eu(III)-based hybrid materials. Furthermore, the synthesized Eu(tfc)$_3$(TPPO-Si)$_2$-SiO$_2$ also showed extra-large intrinsic emission quantum yield (54%), although for the precursor Eu(tfc)$_3$[TPPO-Si(OEt)$_3$]$_2$ was found to be 39%. In the present work, conceptual two-legs standing-up molecular design for bright luminescent Ln(III)-silica nanomaterials is demonstrated for the first time.

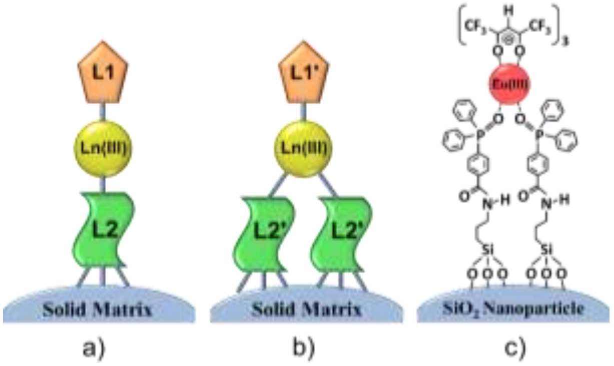

Figure 1. Ln(III) complexes immobilized on the solid matrix with a) one binding site and b) two binding sites. c) Eu(hfa)$_3$ complex with TPPO-Si(OEt)$_3$ ligand covalently bonded to the silica matrix via two binding sites.

Results and Discussion

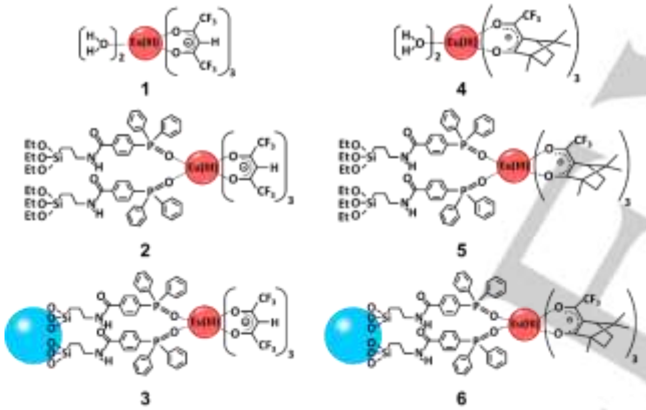

Figure 2. Chemical structures of the compounds that used in this study.

Preparation of nano-luminophore Eu(hfa)$_3$(TPPO-Si)$_2$-SiO$_2$.

The linker ligand for fixation on the SiO$_2$ nanoparticles, triphenylphosphine oxide compound, TPPO-Si(OEt)$_3$, was synthesized according to the procedure in Scheme S1. We used diphenyl(p-tolyl)phosphine as a starting compound and oxidized it with potassium permanganate, the achieved 4-(diphenylphosphino) benzoic acid can be isolated as white crystals from ethanol solution (Figure S1). Then, reaction of 4-(diphenylphosphino) benzoic acid in thionyl chloride with 3-aminopropyl triethoxysilane results in the product of TPPO-Si(OEt)$_3$. The structure was characterized using ^{1}H, ^{31}P, and ^{29}Si NMR spectroscopies, respectively (Figure S2). Previous organosilane compounds have been reported as yellow oils.[42-44] We successfully removed the yellow impurities and obtained a colorless single-crystals for X-ray analysis from the ethyl acetate/hexane solution. The crystal of TPPO-Si(OEt)$_3$ is in monomeric form (Figure 3), which can attach with Eu(III) complex, effectively. Generally, the Eu(hfa)$_3$ binded with two TPPO units,[40] and the TPPO-Si(OEt)$_3$ coordination in Eu(III) can play a role in double-binding sites on the SiO$_2$ nanoparticles.

Concerning the synthesis of lanthanide complex functionalized hybrid materials, two fixation processes were reported: route 1: lanthanide complex with linker is directly attached on the solid matrix; route 2: lanthanide complex is fixed on the linker-modified solid matrix.[45,46] In this study, ethyl groups in the linker ligand TPPO-Si(OEt)$_3$ are easily removed under the coordination reaction with Eu(III) complex in solution. From this reaction condition, we selected the route 2: using Eu(III) complex Eu(hfa)$_3$(H$_2$O)$_2$ (**1**) fixed on the TPPO-Si(OEt)$_3$ modified SiO$_2$ nanoparticles in ethanol solution (Scheme S2). In addition, complex Eu(hfa)$_3$[TPPO-Si(OEt)$_3$]$_2$ (**2**) was also prepared (Scheme S3) for comparison with the target nano-luminophore Eu(hfa)$_3$(TPPO-Si)$_2$-SiO$_2$ (**3**) (Figure 2).

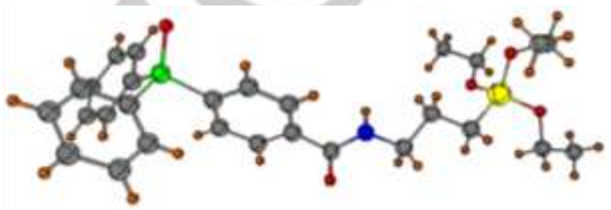

Figure 3. X-ray crystal structure of the triphenylphosphine oxide compound Ph$_2$POC$_6$H$_4$CONH(CH$_2$)$_3$Si(OEt)$_3$ (TPPO-Si(OEt)$_3$).

Characterizations

Dynamic light scattering (DLS) detection showed average size of the prepared silica nanoparticles is 36 nm (Figure 4a), which is in agreement with previously reported result.[47] After modification with Eu(III) complexes, the resulting nano-luminophore **3** displayed an average size of 53 nm (Figure 4b). To get a further understanding of **3** at the nanometre scale, we performed the transmission electron microscopy (TEM) investigation. TEM images revealed particle size of the pure silica nanoparticles (average size around 36 nm, Figure 4c) well-agrees with the DLS result, and energy dispersive X-ray spectroscopy (EDS) confirmed the presence of oxygen and silicon element in the nanoparticles (Figure S3). Significantly different from the pure silica nanoparticles, TEM images of nano-luminophore **3** contained numerous dark objects (Figure 4d). The objects with large size attribute to the Eu(hfa)$_3$(TPPO-Si)$_2$ aggregates on the SiO$_2$ surface, the others are too small to see clearly belong to the Eu(hfa)$_3$(TPPO-Si)$_2$ dispersion functionalized on the silica nanoparticles (Figure S4). Compared with pure SiO$_2$, EDS showed the presence of additional europium, phosphorus and fluorine element in the nano-luminophore **3** (Figure S5), indicated it was constructed by both Eu(hfa)$_3$(TPPO-Si)$_2$ and silica nanoparticles. In the EDS, europium exhibited different species, due to the outer shell electron can come from different shells with different energy. Furthermore, we measured X-ray photoelectron spectroscopy (XPS) of nano-luminophore **3** (Figure S6). In the XPS spectrum, the Eu 3d (5/2) bands corresponding to Eu(III) were observed at 1135 and 1165 eV, which is similar to previously reported simple Eu(III) compounds,[48] confirmed the Eu(hfa)$_3$ is one component of nano-luminophore **3**, consistent with the EDS result.

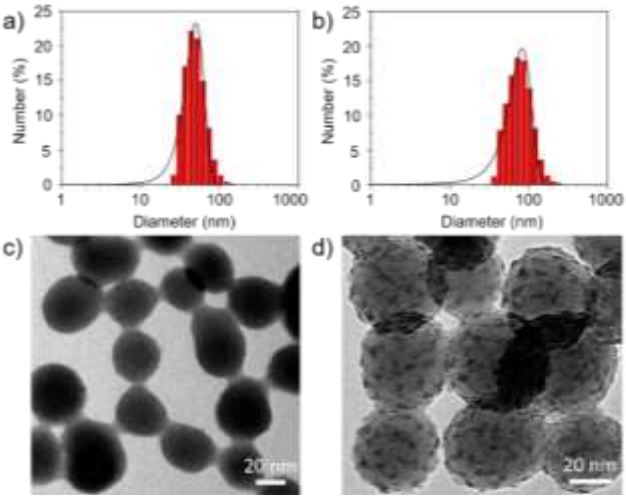

Figure 4. Size distributions of a) pure SiO_2 and b) $Eu(hfa)_3(TPPO\text{-}Si)_2\text{-}SiO_2$ (**3**). TEM images of c) pure SiO_2 and d) $Eu(hfa)_3(TPPO\text{-}Si)_2\text{-}SiO_2$ (**3**).

To investigate the tight-binding between $Eu(hfa)_3$ and $TPPO\text{-}Si(OEt)_3$ modified SiO_2 nanoparticles, we carried out IR measurements. The P=O stretching vibration bands of $TPPO\text{-}Si(OEt)_3$, Eu(III) complex **2** and nano-luminophore **3** are shown in Figure 5. Free organic ligand $TPPO\text{-}Si(OEt)_3$ displays a P=O stretching vibration at 1184 cm^{-1} (Figure 5, black line).[49] However, for complex **2** and nano-luminophore **3** the P=O bands were observed at 1142 cm^{-1} (Figure 5, red and blue lines). The P=O stretching vibrational energy in metal coordination compound is generally smaller than that in non-coordinated organic ligand,[50] indicating the P=O group in nano-luminophore **3** is directly connected with the $Eu(hfa)_3$ unit. In addition, we observed the disappearance of characteristic $-CH_3$ vibrational bands at around 3000 cm^{-1} in nano-luminophore **3** due to the elimination of ethyl groups for connection on SiO_2 surface.

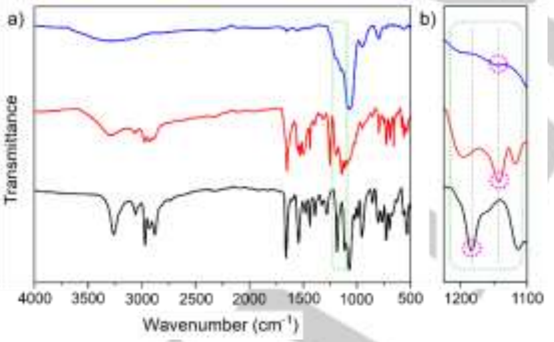

Figure 5. a) FT-IR spectra of $TPPO\text{-}Si(OEt)_3$ (black line), $Eu(hfa)_3[TPPO\text{-}Si(OEt)_3]_2$ (**2**) (red line) and $Eu(hfa)_3(TPPO\text{-}Si)_2\text{-}SiO_2$ (**3**) (blue line). b) Expanded IR spectra for P=O vibrational frequencies.

Further NMR spectroscopy also reveals the evidence for connection between $Eu(hfa)_3$ unit and the $TPPO\text{-}Si(OEt)_3$ modified SiO_2 nanoparticles. In deuterated chloroform, the free $TPPO\text{-}Si(OEt)_3$ displayed a sharp ^{31}P NMR signal at 29.4 ppm (Figure S6). However, after it reacted with the dehydrated $Eu(hfa)_3(H_2O)_2$, the resulting Eu(III) complex **2** exhibited one broad ^{31}P NMR signal at -90.5 ppm (Figure S7), due to the NMR signal is strongly affected by the paramagnetism of the central Eu(III), consistent with previously reported phosphine oxide Eu(III) complex.[51-53] Furthermore, ^{1}H NMR signals of the free ethyl groups come from $TPPO\text{-}Si(OEt)_3$ modified SiO_2 nanoparticles in CD_3OD were also detected (Figure S8), consistent with the IR result that showed disappearance of characteristic $-CH_3$ vibrational bands. Based on the TEM, IR and NMR results, unambiguously indicate that $Eu(hfa)_3$ units were tight-fixed on the TPPO-Si-modified SiO_2 nanoparticles.

To estimate the thermal stability of complex **2** and nano-luminophore **3**, we performed the thermogravimetric analysis (TGA). TGA curve showed the decomposition temperature of complex **2** was 191 °C (Figure S9). On the other hand, decomposition temperature for the nano-luminophore **3** was 282 °C. Significant covalent rigid Si-O-Si polymeric network structures between $Eu(hfa)_3(TPPO\text{-}Si)_2$ units and the silica nanoparticles promote thermo-stable structure under heat-treatment.[54]

Photophysical Properties

Emission spectra of Eu(III) complex **1**, **2** and nano-luminophore **3** were excited at 350 nm (Figure 6), which at the end absorption of the hfa ligand (Figure S10), indicate the hfa can transfer energy efficiently to the central Eu(III). The emission bands observed at 579, 593, 614, 652, and 699 nm, attributed to the Eu(III) ion $^{5}D_0 \rightarrow {}^{7}F_j$ (j = 0 - 4) transitions. Emission spectra are normalized with respect to the magnetic dipole transition intensities at 593 nm (Eu: $^{5}D_0\text{-}{}^{7}F_1$), which is known to be insensitive to the surrounding environment of the lanthanide ions.[40] The characteristic of Eu(III) red luminescence is corresponding to the strongest sharp emission band at 614 nm ($^{5}D_0 \rightarrow {}^{7}F_2$) due to the electric dipole transition, and shape of this transition band is generally affected by coordination environment of the central Eu(III).[55] Relative emission intensity of nano-luminophore **3** is larger than the precursor Eu(III) complex **1** and **2**. The effective large transition band of nano-luminophore **3** is linked with a large radiative rate constant based on the asymmetric coordination structure on the SiO_2 surface. According to the emission spectrum, the splitting shape of the band at 614 nm for complex **2** is similar to nano-luminophore **3**, but significantly different from complex **1**, and the transition intensity is depended on the electric transition probability. Based on these photophysical findings, we consider that in the nano-luminophore **3** $Eu(hfa)_3$ uints are attached by two TPPO units linked with SiO_2.

Emission lifetimes were determined from the slopes of logarithmic plots of the decay profiles (Figure S11). The lifetime corresponding to Eu(III) complex **1**, **2**, and nano-luminophore **3** in solid state were calculated to be 0.42, 0.74, and 0.98 ms, respectively (Table S2). Two components of emission lifetimes for nano-luminophore **3** were estimated as 0.74 and 1.15 ms, the two emission centers should originate from luminescence of the single- and aggregate-Eu(III) complex units on the SiO_2 surface. Emission lifetime for nano-luminophore **3** is much larger than the corresponding complex **1**, **2** and Eu(III)-based singly anchoring hybrid materials (Table S3).[34,38,46] Furthermore, to compare with the nano-luminophore **3**, we prepared a control sample of $SiO_2@Eu(hfa)_3(TPPO)_2$ (mixture of SiO_2 nanoparticles and $Eu(hfa)_3(TPPO)_2$ complex).

Table 1. Photophysical properties of Eu(III) complexes in solid.

Samples		τ_{obs} ^{a} / ms	k_r / s^{-1}	k_{nr} / s^{-1}	Φ_{ff} ^{b} / %	Φ_{tot} ^{c} / %	η_{sens} ^{d} / %
$Eu(hfa)_3(H_2O)_2$	(**1**)	0.42	5.9×10^2	1.8×10^3	25	9	36
$Eu(hfa)_3(TPPO\text{-}Si(OEt)_3)_2$	(**2**)	0.74	7.8×10^2	5.8×10^2	58	31	53
$Eu(hfa)_3(TPPO\text{-}Si)_2\text{-}SiO_2$	(**3**)	0.98	9.5×10^2	6.9×10	93	27	29
$Eu(tfc)_3(H_2O)_2$	(**4**)	0.16	5.93×10^2	5.78×10^3	9	- ^{e}	-
$Eu(tfc)_3[TPPO\text{-}Si(OEt)_3]_2$	(**5**)	0.42	9.40×10^2	1.46×10^3	39	9	23
$Eu(tfc)_3(TPPO\text{-}Si)_2\text{-}SiO_2$	(**6**)	0.50	1.07×10^3	9.20×10^2	54	5	9

[a] λ_{ex} = 356 nm. [b] Caclulation method is shown in exprimental section. [c] λ_{ex} = 320 nm. [d] The photosensitized energy transfer efficiency $\eta_{sens} = \Phi_{tot} / \Phi_{ff}$. [e] The value is too low to collect.

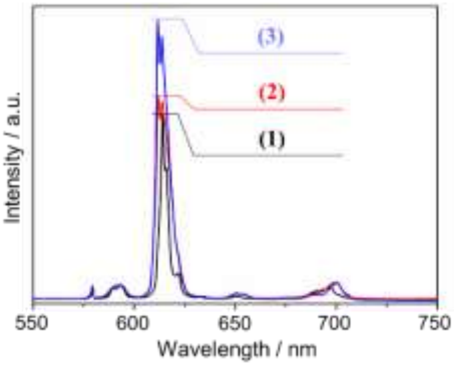

Figure 6. Emission spectra of $Eu(hfa)_3(H_2O)_2$ (**1**) (black line), $Eu(hfa)_3[TPPO\text{-}Si(OEt)_3]_2$ (**2**) (red line) and $Eu(hfa)_3(TPPO\text{-}Si)_2\text{-}SiO_2$ (**3**) (blue line), which were excited at 350 nm in solid state at room temperature.

When the $SiO_2@Eu(hfa)_3(TPPO)_2$ was washed four times with diethyl ether, resulting in non-emissive powders without $Eu(hfa)_3(TPPO)_2$ (Table S4). These results clearly revealed that the lifetime enhancement of nano-luminophore **3** due to the $Eu(hfa)_3(TPPO\text{-}Si)_2$ complex covalently bonded to the silica matrix.

Emission lifetimes, emission quantum yields, radiative and non-radiative rate constants were summarized in Table 1.[56] The nano-luminophore **3** exhibits an extra-large intrinsic emission quantum yield ($\Phi_{ff,}$ 93%), higher than the precursor Eu(III) complex **1** and **2**. This Φ_{ff} is based on a large radiative rate constant (k_r, 9.5×10^2 s^{-1}) and an extremely small non-radiative rate constant (k_{nr}, 6.9×10 s^{-1}). The k_{nr} is smaller than those previously reported Eu(III) complex with phosphine oxide, naphthalene, and pyridine ligands (10^2 s^{-1}).[57-59] The large k_r for nano-luminophore **3** should be due to tight and antisymmetric aggregations of the $Eu(hfa)_3(TPPO\text{-}Si)_2$ units on the silica nanospheres (Scheme S5). Suppression of k_{nr} of nano-luminophore **3** is achieved using the $TPPO\text{-}Si(OEt)_3$ ligand bonded on the silica nanoparticles. It can be attributed to the following reasons: (i) the organic ligand $TPPO\text{-}Si(OEt)_3$ has a three-dimensional antisymmetric structure that promotes faster radiative rate and suppresses non-radiative rate; (ii) in the nano-luminophore **3**, the covalent rigid Si-O-Si polymeric network structures restrict the thermal-vibrations of $TPPO\text{-}Si(O)_3$ ligand.[54] The Φ_{ff} of nano-luminophore **3** is significantly higher than previously reported Eu@Si-OH (38%)[60] (which is the $Eu(TPPO)_2$ with one bidentate anchored on the silica nanoparticles), and Eu(III)-based materials such as Eu(III)-SBA-15 (29%),[34] Eu(III)-MCM-41 (81%),[35] Dpdp-ePMO-$Eu(tta)_3$ (7.5%)[37] and even larger than the pure Eu(III) complex with phosphine oxide and pyridine ligand[41,61-63]. In addition, the photosensitized energy transfer efficiency η_{sens} for nano-luminophore **3** was estimated to be 29%, which is smaller than Eu(III) complex **1** and **2**. The η_{sens} might be related to excited triplet-state lifetime. To get a further understanding of the energy transfer efficiency observed for complex **2** and **3**, we investigated lifetime of the corresponding gadolinium complex at 90K (Table S5). The average triplet-state lifetime of hfa ligand in $Gd(hfa)_3(TPPO\text{-}Si)_2\text{-}SiO_2$ is 15 ms, which is smaller than those of in the $Gd(hfa)_3[TPPO\text{-}Si(OEt)_3]_2$ (47 ms), in agreement with their energy transfer efficiency in complex **2** and nano-luminophore **3**.

Using organic ligand $TPPO\text{-}Si(OEt)_3$ as support, we developed a nano-luminophore **3**, which shows larger emission quantum yield than those of previous reported Eu(III)-coordinated materials, suggesting $TPPO\text{-}Si(OEt)_3$ is a promising candidate for the development of Eu(III)-based luminescent nanomaterials. To verify this supposition, we prepared the Eu(III) complex $Eu(tfc)_3(H_2O)_2$ (**4**), $Eu(tfc)_3[TPPO\text{-}Si(OEt)_3]_2$ (**5**) and hybrid nano-luminophore $Eu(tfc)_3(TPPO\text{-}Si)_2\text{-}SiO_2$ (**6**) (Figure 2). The relative emission intensity of the $^5D_0 \rightarrow {}^7F_2$ transition for nano-luminophore **6** is higher than Eu(III) complex **4** and **5** (Figure S13), in agreement with their observed luminescence lifetimes (Table S6). Furthermore, the nano-luminophore **6** provides larger Φ_{ff} (54%) than complex **5** (39%) and **4** (9%) (Table 1). This large Φ_{ff} is also based on a higher radiative rate constant (k_r, 1.07×10^3 s^{-1}) and a lower non-radiative rate constant (k_{nr}, 9.20×10^2 s^{-1}). Compare with complex **5**, the nano-luminophore **6** has a lower photosensitized energy transfer efficiency. The low η_{sens} for nano-luminophore **6** (9%) and **3** (29%) might be related to the stabilization of the excited triplet states of tfc and hfa ligand. Depending on the phosphorescence lifetime of $Gd(hfa)_3(TPPO\text{-}Si)_2\text{-}SiO_2$ (ave. lifetime = 15 ms) is smaller than that of $Gd(hfa)_3[TPPO\text{-}Si(OEt)_3]_2$ (ave. lifetime = 47 ms), we consider that the unstable excited-triplet state of hfa and tfc ligand in nano-luminophore **3** and **6** promote their lower photosensitized energy transfer efficiency.

According to the above results, the triphenylphosphine oxide compound $TPPO\text{-}Si(OEt)_3$ can act as a support covalent on the silica nanoparticles. In the case of hfa and tfc as photosensitization ligand, the achieved Eu(III) coordinated nano-luminophore **3** and **6** exhibit large intrinsic quantum yield and long emission lifetime than the corresponding pure Eu(III) complex.

Conclusions

A novel triphenylphosphine oxide compound TPPO-Si(OEt)$_3$ was synthesized for fixation of Eu(III) complex on the nano-silica surface. Using Eu(hfa)$_3$ complex with TPPO-Si(OEt)$_3$ ligand covalently bonded to the silica nanoparticles through two binding sites, we developed a nano-luminophore Eu(hfa)$_3$(TPPO-Si)$_2$-SiO$_2$ (**3**) with excellent intrinsic luminescence quantum yield and long emission lifetime, due to the covalent rigid Si-O-Si polymeric network structure that formed on the silica nanoparticles surface restricts the vibration of the organic ligand. The emission quantum yield of doubly anchoring Eu(hfa)$_3$(TPPO-Si)$_2$-SiO$_2$ is much larger than those of singly anchoring Eu(III) compounds on SiO$_2$ (Table S4). In the case of tfc as effective photosensitization ligand, we also confirmed the TPPO-Si(OEt)$_3$ is an excellent candidate for developing Eu(III)-functionalized hybrid luminescent materials. This general methodology using TPPO-Si(OEt)$_3$ as the support to develop Eu(III)-coordinated nanomaterials can apply to other lanthanide (Tb, Dy) complexes and silica matrices (mesoporous silica materials, micro silica particles, silica glass materials), opening their corresponding application as luminescent materials.

Deposition Numbers 2045883 (for TPPO-Si(OEt)$_3$) contain the supplementary crystallographic data for this paper. These data are provided free of charge by the joint Cambridge Crystallographic Data Centre and Fachinformationszentrum Karlsruhe Access Structures service www.ccdc.cam.ac.uk/structures.

Acknowledgements

This work was supported by Grant-in-Aid for Grant Number JP20K21201, JP20H05197, JP20H04653, JP20H02748, JP19H04556, JP18H04497 and JP18H02041. This work was also supported by the Institute for Chemical Reaction Design and Discovery (ICReDD), established by the World Premier International Research Initiative (WPI) of MEXT, Japan.

Keywords: europium complex • nanoparticles • luminescence

[1] J. Silver, R. Withnall, Luminescent Materials and Applications; Kitai, A., Ed.; John Wiley & Sons: Chicester, **2008**.
[2] Y. Zhang, J. Hao, *J. Mater. Chem. C* **2013**, *1*, 5607-5618.
[3] H. Dong, S.-R. Du, X.-Y. Zheng, G.-M. Lyu, L.-D. Sun, L.-D. Li, P.-Z. Zhang, C. Zhang, C.-H. Yan, *Chem. Rev.* **2015**, *115*, 10725-10815.
[4] J. Zhou, Q. Liu, W. Feng, Y. Sun, F. Li, *Chem. Rev.* **2015**, *115*, 395-465.
[5] W. P. Lustig, S. Mukherjee, N. D. Rudd, A. V. Desai, J. Li, S. K. Ghosh, *Chem. Soc. Rev.* **2017**, *46*, 3242-3285.
[6] H. Zollinger, Color Chemistry: Syntheses, Properties, and Applications of Organic Dyes, Pigments, 3rd ed.; Wiley-VCH: Weinheim, **2003**, pp. 15-50.
[7] H. Kobayashi, M. Ogawa, R. Alford, P. L. Choyke, Y. Urano, *Chem. Rev.* **2010**, *110*, 2620-2640.
[8] Q. Zhao, C. H. Huang, F. Y. Li, *Chem. Soc. Rev.* **2011**, *40*, 2508-2524.
[9] D. L. Ma, H. Z. He, K. H. Leung, D. S. H. Chan, C. H. Leung, *Angew. Chem. Int. Ed.* **2013**, *52*, 7666-7682.
[10] J.-C. G. Bünzli, *Chem. Rev.* **2010**, *110*, 2729-2755.
[11] J.-C. G. Bünzli, *Coord. Chem. Rev.* **2015**, *293*, 19-47.
[12] L. Wang, Z. Zhao, C.; Wei, H. Wei, Z. Liu, Z. Bian, C. Huang, *Adv. Opt. Mater.* **2019**, *7*, 1801256.
[13] K. Binnemns, *Chem. Rev.* **2009**, *109*, 4283-4374.
[14] K. M. L. Taylor-Pashow, J. D. Rocca, R. C. Huford, W. Lin, *Chem. Commun.* **2010**, *46*, 5832-5849.
[15] L. Li, W. Wang, J. Tang, Y. Wang, J. Liu, L. Huang, Y. Wang, F. Guo, J. Wang, W. Shen, L. A. Belfiore, *Nanoscale Res. Lett.* **2019**, *14*, 190.
[16] X. Liu, J. Iocozzia, Y. Wang, X. Cui, Y. Chen, S. Zhao, Z. Li, Z. Lin, *Energy Environ. Sci.* **2017**,*10*, 402-434.
[17] S. Cousinié, L. Mauline, M. Gressier, S. R. Kandibanda, L. Datas, C. Reber, M.-J. Menu, *New J. Chem.* **2012**, *36*, 1355-1367.
[18] H. Liu, F. Nosheen, X. Wang, Chem. Soc. Rev., 2015, 44, 3056-3078.
[19] T. B. Demille, R. A. Hughes, A. S. Preston, R. Adelung, Y. K. Mishra, S. Neretina, *Front. Chem.* **2018**, *6*, 411-418.
[20] B. Wu, Y. Kuang, X. Zhang, J. Chen, *Nano Today* 2011, *6*, 75-90.
[21] G. Doria, J. Conde, B. Veigas, L. Giestas, C. Almeida, M.; M. Assunção, J. Rosa, P. V. Baptista, *Sensors* **2012**, *12*, 1657-1687.
[22] M. Davidson, Y. Ji, G. J. Leong, N. C. Kovach, B. G. Trewyn, R. M. Richards, *ACS Appl. Nano Mater.* **2018**, *1*, 4386-4400.
[23] H. Chen, X. Yang, Y. Liu, L. Wang, *Anal. Bioanal. Chem.* **2020**, *412*, 5843-5851.
[24] M. L. Rosa, S. A. Denisov, G. Jonusauskas, N. D. McClenaghan, A. Credi, *Angew. Chem. Int. Ed.* **2018**, *57*, 3104-3107.
[25] T. Zhao, J. Han, X. Jin, Y. Liu, M. Liu, P. Duan, *Angew. Chem. Int. Ed.* **2019**, *58*, 4978-4982.
[26] S. V. Eliseeva, J.-C. G. Bünzli, *Chem. Soc. Rev.* **2010**, *39*, 189-227.
[27] K. P. S. Zanoni, L. P. Ravaro, A. S. S. Camargo, *Dalton Trans.* **2018**, *47*, 12813-12826.
[28] J. Feng, H. Zhang, *Chem. Soc. Rev.* **2013**, *42*, 387-410.
[29] H. Li, P. Li, *Chem. Commun.* **2018**, *54*, 13884-13893.
[30] A. M. Kaczmarek, P. V. D. Voort, *Materials* **2020**, *13*, 566-591.
[31] K. Lunstroot, K. Driesen, P. Nockemann, L. Viau, P. H. Mutin, A. Vioux, K. Binnemans, *Phys. Chem. Chem. Phys.* **2010**, *12*, 1879-1885.
[32] M. Martínez-Calvo, O. Kotova, M. E. Möbius, A. P. Bell, T. McCabe, J. J. Boland, T. Gunnlaugsson, *J. Am. Chem. Soc.* **2015**, *137*, 1983-1992.
[33] P. Chen, Q. Li, S. Grindy, N. Holten-Andersen, *J. Am. Chem. Soc.* **2015**, *137*, 11590-11593.
[34] Y. Li, B. Yan, H. Yang, *J. Phys. Chem. C* **2008**, *112*, 3959-3968.
[35] D. B. A. Raj, S. Biju, M. L. P. Reddy, *J. Mater. Chem.* **2009**, *19*, 7976-7983.
[36] A. Gulino, F. Lupo, G. G. Condorelli, A. Motta, I. L. Fragalà, *J. Mater. Chem.* **2009**, *19*, 3507-3511.
[37] D. Esquival, A. M. Kaczmarek, C. Jiménez-Sanchidrián, R. V. Deun, F. J. Romero-Salguero, P. V. D. Voort, *J. Mater. Chem. C* **2015**, *3*, 2909-2917.
[38] X. Pang, L. Li, Y. Wei, X. Yu, Y. Li, *Dalton Trans.* **2018**, *47*, 11530-11538.
[39] Y. Hasegawa, Y. Kimura, K. Muakoshi, Y. Wada, J.-H. Kim, N. Nakashima, T. Yamanaka, S. Yanagida, *J. Phys. Chem.* **1996**, *100*, 10201-10205.
[40] Y. Hirai, T. Nakanishi, Y. Kitagawa, K. Fushimi, T. Seki, H. Ito, Y. Hasegawa, *Angew. Chem. Int. Ed.* **2016**, *55*, 12059-12062.
[41] A. Nakajima, T. Nakanishi, Y. Kitagawa, T. Seki, H. Ito, K. Fushimi, Y. Hasegawa, *Sci. Rep.* **2016**, *6*, 24458-24466.
[42] S. Titos-Padilla, E. Colacio, S. J. A. Pope, J. J. Delgado, M. Melgosa, J. M. Herrera, *J. Mater. Chem. C* **2013**, *1*, 3808-3815.
[43] A.-C. Franville, D. Zambon, R. Mahiou, *Chem. Mater.* **2000**, *12*, 428-435.
[44] L. Wang, A. Reis, A. Seifert, T. Philippi, S. Ernst, M. Jia, W. R. Thiel, *Dalton Trans.* **2009**, 3315-3320.
[45] S. Cousinié, M. Gressier, C. Reber, J. Dexpert-Ghys, M.-J. Menu, *Langmuir* **2008**, *24*, 6208-6214.
[46] A. P. Duarte, M. Gressier, M.-J. Menu, J. Dexpert-Ghys, J. M. A. Caiut, S. J. L. Ribeiro, *J. Phys. Chem. C* **2012**, *116*, 505-515.
[47] C. Hübner, C. Fettkenhauer, K. Voges, D. C. Lupascu, *Langmuir* **2018**, *34*, 376-383.

[48] S. Thongchant, S. Katagiri, Y. Hasegawa, Y. Wada, S. Watase, M. Nakamoto, T. Sakata, H. Mori, S. Yanagida, *Bull. Chem. Soc. Jpn.* **2004**, *77*, 807‑812.

[49] M. Halmann, S. Pinchas, *J. Chem. Soc.* **1958**, 3264-3267.

[50] E. Giesbrecht, *Pure & Appt. Chem.* **1979**, *51*, 925-947.

[51] F. Embert, A. Mehdi, C. Reyé, R. J. P. Corriu, *Chem. Mater.* **2001**, *13*, 4542-4549.

[52] H. Iwanaga, *Bull. Chem. Soc. Jpn.* **2019**, *92*, 1385-1393.

[53] N. B. D. Lima, S. M. C. Gonçalves, S. A. Júnior, A. M. Simas, *Sci. Rep.* **2013**, *3*, 2395.

[54] Y. Wanga, B. Li, L. Zhang, Q. Zuo, L. Liu, P. Li, *J. Colloid Interface Sci.* **2010**, *349*, 505-511.

[55] Y. Kuramochi, T. Nakagawa, T. Yokoo, J. Yuasa, T. Kawaia, Y. Hasegawa, *Dalton Trans.* **2012**, *41*, 6634-6640.

[56] M. H. V. Werts, R. T. F. Jukes, J. W. Verhoeven, *Phys. Chem. Chem. Phys.* **2002**, *4*, 1542-1548.

[57] Y. Kitagwa, F. Suzue, T. Nakanishi, K. Fushimi, Y. Hasegawa, *Dalton Trans.* **2018**, *47*, 7327-7332.

[58] T. Koizuka, M. Yamamoto, Y. Kitagawa, T. Nakanishi, K. Fushimi, Y. Hasegawa, *Bull. Chem. Soc. Jpn.* **2017**, *90*, 1287-1292.

[59] M. R. Felício, T. G. Nunes, P. M. Vaz, A. M. P. Botas, P. Ribeiro-Claro, R. A. S. Ferreira, R. O. Freire, P. D. Vaz, L. D. Carlos, C. D. Nunes, M. M. Nolasco, *J. Mater. Chem. C* **2014**, *2*, 9701-9711.

[60] B. Francis, B. Neuhaus, M.L.P. Reddy, M. Epple, C. Janiak, *Eur. J. Inorg. Chem.* **2017**, *25*, 3205-3213.

[61] O. Moudam, B. C. Rowan, M. Alamiry, P. Richardson, B. S. Richards, A. C. Jones, N. Robertson, *Chem. Commun.* **2009**, 6649-6651.

[62] J. M. Stanley, X. Zhu, X. Yang, B. J. Holliday, *Inorg. Chem.* **2010**, *49*, 2035-2037.

[63] C. R. D. Silva, J. R. Maeyer, R. Wang, G. S. Nichol, Z. Zheng, *Inorganica Chim. Acta* **2007**, *360*, 3543-3552.

Entry for the Table of Contents

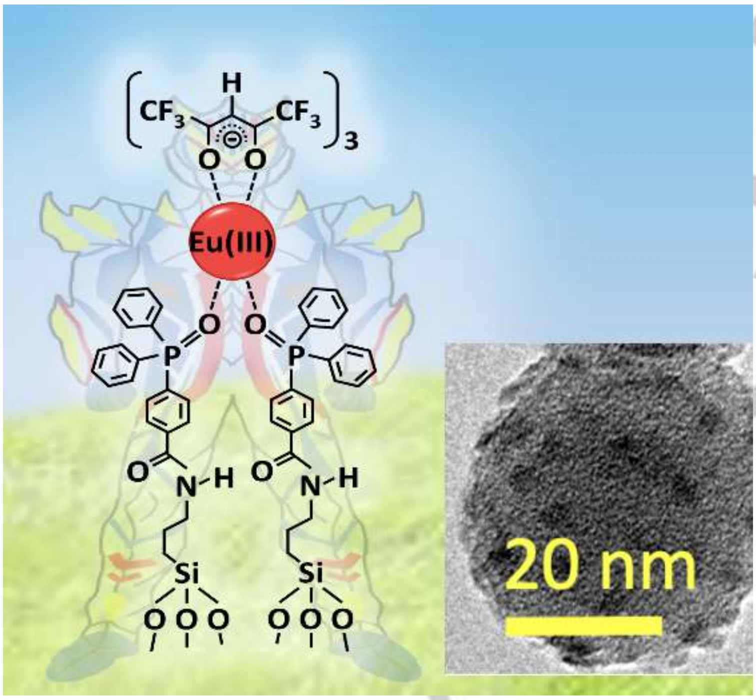

A novel method for development of lanthanide-based hybrid nanomaterials, taking advantage of an Eu(III) complex with organic ligand covalently bonded to the silica nanoparticles through two binding sites as support was demonstrated. The developed hybrid nano-luminophore exhibited higher intrinsic luminescence quantum yield (93%) and longer emission lifetime (0.98 ms), which is much larger than those of previous Eu(III)-based hybrid materials.